

Incorporation of laser-induced graphene with hierarchical NiCo layered double hydroxide nanosheets for electrochemical determination of glucose in food and serum

Peer-reviewed author version

Huang, Man; Ye, Lei; Yu, Liwen; Zhang , Yuanyuan; Zeng, Ting; Yang , Juan; Tian , Fan; Wu, Zhen; Zhang , Xiuhua; Hu, Chengguo & YANG, Nianjun (2024)

Incorporation of laser-induced graphene with hierarchical NiCo layered double hydroxide nanosheets for electrochemical determination of glucose in food and serum. In: *Analytica chimica acta*, 1329 (Art N° 343194).

DOI: 10.1016/j.aca.2024.343194

Handle: <http://hdl.handle.net/1942/44444>

# **Incorporation of laser-induced graphene with hierarchical NiCo layered double hydroxide nanosheets for electrochemical determination of glucose in food and serum**

Man Huang,<sup>a</sup> Lei Ye,<sup>a</sup> Liwen Yu,<sup>a</sup> Yuanyuan Zhang,<sup>a,\*</sup> Ting Zeng,<sup>a</sup> Juan Yang,<sup>a</sup> Fan Tian,<sup>a</sup> Zhen Wu,<sup>b</sup> Xiuhua Zhang,<sup>b</sup> Chengguo Hu,<sup>c</sup> Nianjun Yang<sup>d</sup>

<sup>a</sup>School of Chemistry and Environmental Engineering, School of Materials Science and Engineering, Key Laboratory of Green Chemical Engineering Process of Ministry of Education, Hubei Key Laboratory of Novel Reactor and Green Chemical Technology, Wuhan Institute of Technology, Wuhan 430205, China.

<sup>b</sup>Hubei Collaborative Innovation Center for Advanced Organic Chemical Materials, Ministry of Education Key Laboratory for the Synthesis and Application of Organic Functional Molecules, College of Chemistry and Chemical Engineering, Hubei University, Wuhan, 430062, PR China.

<sup>c</sup>College of Chemistry and Molecular Sciences, Wuhan University, Wuhan 430072, China

<sup>d</sup>Department of Chemistry & IMO-IMOMEC, Hasselt University Diepenbeek 3590, Belgium.

\*Corresponding author e-mail: [yyzhang@wit.edu.cn](mailto:yyzhang@wit.edu.cn) (Y. Zhang)

**Abstract** Dependable and sensitive glucose (Glu) testing in foodstuff and blood serum is highly desirable to prevent and treat diabetes. Electrochemical quantification of Glu has attracted great interests due to the advantages, including simple operation, higher sensitivity, easy miniaturization, ease of on-site and wearable detection as well as fast response. High costs and environmental dependence of enzymes pose a challenge to the electrochemical enzymatic biosensors. Nonenzymatic electrochemical Glu sensors are urgently needed to aid the Glu detection in human serum and food samples. To fabricate flexible Glu electrochemical sensors, designing suitable electrode substrate and efficient electrocatalyst is of paramount significance. Herein, the porous patterned laser-induced graphene (LIG) was fabricated on polyimide substrates through an efficient laser-inducing technology, and then used

directly as the electrode substrate. Electrochemical deposition of NiCo layered double hydroxide (LDH) nanoflakes on the LIG surface was then conducted to achieve NiCo-LDH/LIG electrode as a Glu sensor. Under optimal conditions, this sensor displays a low detection limit of 0.05  $\mu\text{M}$ . Two sets of broad detection linear ranges were found to be from 0.5 to 270  $\mu\text{M}$  and from 0.27 to 3.6 mM, with high sensitivities of 9.750  $\mu\text{A } \mu\text{M}^{-1} \text{ cm}^{-2}$  and 3.760  $\mu\text{A } \mu\text{M}^{-1} \text{ cm}^{-2}$ , respectively. The enhanced performance was ascribed to the cooperative action of NiCo-LDH and LIG, in which porous LIG provides extraordinary electroconductibility and a high surface area, while NiCo-LDH offers numerous exposed active sites and outstanding electrocatalytic performance. Practical application was further verified during the Glu detection in human serum and food samples. This research confirms that the NiCo-LDH/LIG composite is a prospective electrode for high-performance Glu sensor and provides a way of developing nonenzymatic electrochemical sensors to analyze the Glu in human serum and food samples, opening new avenues in electrochemical sensing.

**Keywords:** Electrochemical sensor; Glucose; Laser-induced graphene (LIG); NiCo-LDH; Nonenzymatic sensing

## 1. Introduction

Diabetes is a well-known metabolic disease due to glucose (Glu) metabolic disorder (i.e., high blood Glu levels) which may cause severe health problems [1]. Over 500 million people around the world endure diabetes mellitus and this number is growing rapidly in recent years. On the other hand, Glu balances sweetness and improves tastes. It is then frequently added to various foodstuffs (e.g., beverages, milk and coffee drinks) [2]. Consequently, dependable and sensitive Glu testing in foodstuff and blood serum is highly desirable to prevent and treat diabetes.

Many sensing techniques like surface-enhanced Raman scattering, fluorescence, colorimetry and high-performance liquid chromatography (HPLC) have been employed to monitor Glu and display high sensitivity and precision, but these analysis methods are limited by the lack of simple, budget, and easy-to-use instrumentations as well as the requirement of sophisticated sample pretreatment procedure [3-6]. To manage these technical difficulties, electrochemical quantification of Glu was

developed and has attracted great interests by virtue of its many advantages, including lower cost, simple operation, higher sensitivity and selectivity, easy miniaturization, ease of on-site and wearable detection as well as fast response [7,8]. Electrochemical Glu platforms can be classified into enzymatic and enzyme-free sensors. Originally, the enzymatic type sensors have been used extensively owing to their high selectivity and reliability [9]. Nevertheless, their high costs and environmental dependence of enzymes pose a challenge to the electrochemical enzymatic biosensors [9]. Therefore, many studies have focused on the Glu sensors without the enzyme, which function through direct electrocatalysis of the sensing materials utilized to modify the electrode and direct oxidation of Glu on the electrode surface [10].

For example, tremendous efforts have been done to develop electrocatalysts with prominent electrocatalytic ability for fabricating non-enzymatic Glu sensors. Among them, precious metal nanoparticles (i.e., platinum, gold, silver, and so on.) and their alloys have been widely employed for the non-enzymatic determination of Glu in that they possess a high catalytic activity against Glu [11-14]. Nevertheless, their applications are hindered by their low abundance, easy inactivation, and high costs [15].

Therefore, investigators have been triggered to investigate and develop catalysts with superior electrocatalytic behavior and low costs for Glu electrooxidation. It is worth noting that the first-row transition metal (i.e., Co, Ni, Cu, Fe and Mn) nanoparticles and their oxides, metal-organic frameworks, hydroxides as well as other compounds offer the advantages of low cost, long-term stability, earth abundance, and high activities in electrocatalytic sensing toward Glu electrooxidation, making them promising materials for developing Glu electrochemical sensors [16-20]. Particularly, Ni- and Co- based electrocatalysts have emerged as the most hopeful electrochemical sensing materials for the Glu detection due to their high detection activity. Meanwhile, the merged type of Ni and Co systems can offer the cooperative function toward the electrocatalysis [21,22]. Among these Ni- and Co-containing compounds, layered double hydroxide (LDH) nanosheets are particularly promising in the field of catalysis because of their advantages of outstanding electrocatalytic ability, highly interconnected structure and enhanced redox activity [23-25]. Nevertheless, a LDH possesses low conductive and dielectric properties, which hinders its further adhibition in the field of electrochemical sensor.

To enhance the catalytic performance and electrical conductivity of LDHs, a

preferred approach is to incorporate them with nanocarbons or noble metal nanoparticles which possess excellent electrical conductivity [26,27]. Graphene, as one kind of carbon nanomaterials, is an ideal candidate as the conductive substrate due to its rich surface chemistry, a large accessible surface area and highly conductive character [28]. Although a variety of approaches including chemical vapor deposition, chemical exfoliation and the reduction of graphene oxide (GO) have been successfully employed to prepare graphene [29,30], the conventional synthesis method of graphene suffers from the use of expensive instrument, the application of high temperatures, dangerous and complex handling processes, and time-consuming. By comparison, direct laser writing (DLW) is likely an appropriate technique for graphene synthesis that can resolve the challenges of the aforementioned approaches [31]. It features a one-step, rapid, and reagent-less procedure for graphene preparation under laser irradiation of suitable carbon precursors (e.g., a polyimide (PI) film) [32]. More extraordinarily, DLW enables the construction of three-dimensional (3D) porous and interconnected graphene network, known as laser-induced graphene (LIG) [33].

Thanks to the advantages of superior electrochemical performance and electrocatalytic activity, efficient and cost-effective preparation as well as porous structure with high accessible surface areas, LIG has been employed for some applications containing electrochemical sensor, energy storage and electrocatalysis [34-36]. In addition, the 3D porous graphene can be an interesting supporting structure offering many active sites, coating with other active materials [37]. More importantly, the patterned LIG on the PI sheet can be employed directly as the substrate of a working electrode in place of the usual working electrodes such as glassy carbon electrodes, which lack flexibility and are challenging to fabricate flexible and wearable sensor [38].

In this work, a novel enzyme-free electrochemical Glu sensor (NiCo-LDH/LIG) is constructed by the electrodeposition of NiCo-LDH nanoflakes on a LIG electrode, leveraging their outstanding electrocatalytic properties. The patterned LIG was first produced on the PI film through the laser-induced technology, and then high dense NiCo-LDH nanoflakes were electrodeposited on the LIG surface, gaining a NiCo-LDH/LIG electrode. After being characterized using various techniques, this electrode was utilized for the Glu determination. Stemming from the cooperative features between the 3D porous architecture of the LIG foam and NiCo-LDH nanoflakes, the developed NiCo-LDH/LIG electrode possesses a high electrocatalytic area, rapid

electron transfer, and excellent electrochemical activity for sensing Glu. The established non-enzymatic sensors exhibited the advantages of a linear response in a wide range, high sensitivity, low detection limit, satisfactory selectivity and feasibility in foodstuff and human serum.

## **2. Materials and methods**

### *2.1. Chemicals and reagents*

All chemicals were analytically pure and was utilized without further treatment. Cobalt nitrate hexahydrate ( $\text{Co}(\text{NO}_3)_2 \cdot 6\text{H}_2\text{O}$ ), sodium hydroxide (NaOH), potassium chloride (KCl), nickel nitrate hexahydrate ( $\text{Ni}(\text{NO}_3)_2 \cdot 6\text{H}_2\text{O}$ ), potassium ferricyanide (III) ( $\text{K}_3[\text{Fe}(\text{CN})_6]$ ), citric acid (CA), lactose (Lac), uric acid (UA), sucrose (Suc), ascorbic acid (AA), fructose (Fru), sodium chloride (NaCl), dopamine (DA), and sodium carbonate ( $\text{Na}_2\text{CO}_3$ ) were all procured from Shanghai Sinopharm Chemical Reagent Co., Ltd. The commercial polyimide (PI, Kapton) with a thickness of 0.055 mm was supplied by Shenzhen Xinhongsen Technology Co., Ltd and used as source of graphene. The CheKine Micro Glucose Assay Kit (KTB1300) was purchased from Abbkine Scientific Co., Ltd. (Wuhan, China). All experiments were accomplished in high-purity Milli-Q water.

### *2.2. Instrument*

Specific patterns of LIG were produced utilizing a constant focusing laser (Diaotu Engraving Machine L1, Shanghai Diaotu Tech. Co., Ltd.). A scanning electron microscope (SEM, JEOL-JSM-7100F) was applied to study the morphology and structure of LIG and NiCo-LDH/LIG. With the aid of a transmission electron microscope (TEM, Tecnai G2 20 S-TWIN), the TEM images were gained. The XPS measurements was utilized in the chemical composition investigation and conducted on an AXIS Ultra DLD instrument. Raman measurements were performed adopting a Thermo Fischer DXR Raman microscope. Moreover, the powder X-ray diffraction (XRD) investigations of LIG and NiCo-LDH/LIG were carried out in Bruker AXS D8. All the electrochemical data were collected utilizing a CHI660E electrochemical workstation.

### *2.3. Formation of graphene on PI*

A piece of 0.055 mm thickness PI sheet was utilized as a processing material for

the LIG production. Then, the PI sheet was taped on a PET surface and then subjected to laser-engraving exploiting self-designed one-electrode patterns with a wavelength of 450 nm and a laser peak power of 3.8 W. Afterward, a working area (3 mm in diameter) was defined by an insulating film.

#### 2.4. Fabrication of NiCo-LDH/LIG electrodes

The potentiostatic electrodeposition of NiCo-LDH on LIG was carried out in a standard three-electrode cell. The prepared LIG sheet or the glassy carbon electrode (GCE, diameter = 3 mm) served as the working electrode (WE), a Pt wire as the counter electrode (CE), and a SCE (saturated KCl) as the reference electrode (RE). The three-electrode system was immersed in 10 mL H<sub>2</sub>O containing 8 mM Co(NO<sub>3</sub>)<sub>2</sub> and 2 mM Ni(NO<sub>3</sub>)<sub>2</sub>, and the NiCo-LDH materials were modified on the LIG surface through an electrodeposition process via a potentiostatic mode at -1.0 V for 300 s. After that, the prepared NiCo-LDH/LIG electrode was washed with triple distilled water, and then placed under an infrared lamp. For comparison, NiCo-LDH/GCE were also fabricated under the above conditions. The experiments were performed at room temperature and atmospheric pressure. The preparation procedure of a NiCo-LDH/LIG sensor for quantifying Glu is clarified in Fig. 1.

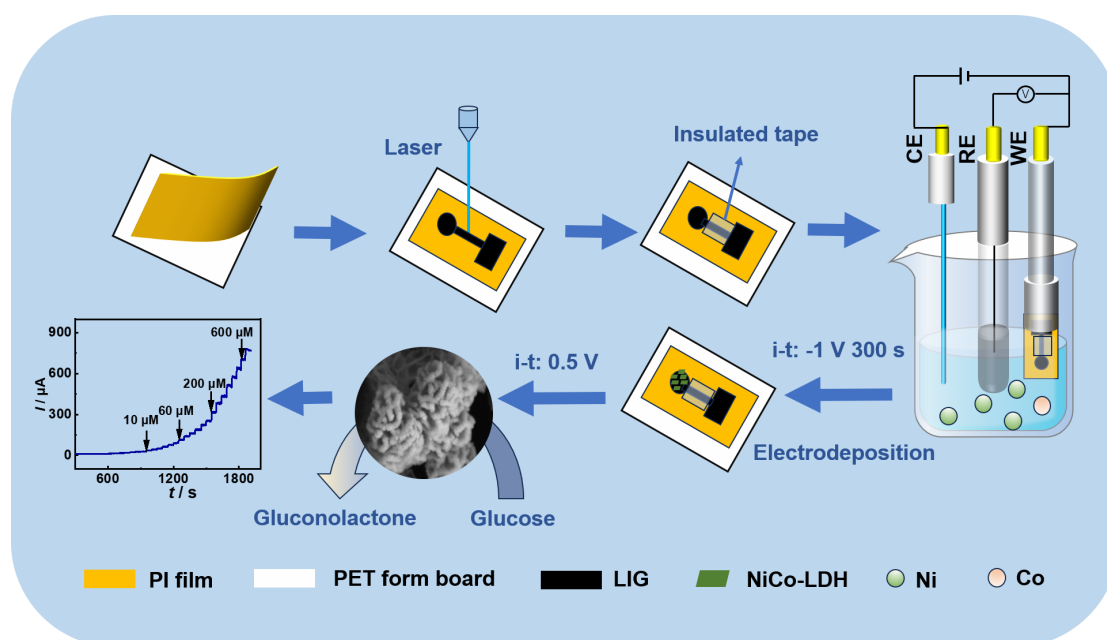


**Figure 1.** Preparation of a NiCo-LDH/LIG electrode through laser-engraving and electrochemical deposition as well as its use in the electrochemical sensing of glucose.

### 2.5. Real sample pretreatment

To assess the practicability of the proposed NiCo-LDH/LIG sensor towards the Glu detection, a series of samples including coffee drinks, milk, milk tea, cola, orange juice, vitamin drinks, honey and human serum were selected as the actual samples. Before detecting the electrochemical signals, these samples were firstly treated. The coffee drinks, milk, cola, orange juice and vitamin drinks were diluted 10 times with water, and then filtered by 0.45  $\mu\text{m}$  membrane filters. For 1.6 g of milk tea powder or 1.6 g of honey samples, it was dissolved in 8 mL  $\text{H}_2\text{O}$  solution, and then filtered by 0.45  $\mu\text{m}$  membrane filters. The serum samples were centrifuged at 8000 rpm for 10 min and then directly used.

## 3. Results and discussion

### 3.1. Physicochemical features of LIG and NiCo-LDH/LIG composites

The surface microstructure and morphology of LIG and NiCo-LDH/LIG composites was investigated by use of SEM and TEM. From the SEM and TEM images of LIG (Fig. 2A and B), the LIG is a honeycomb-like texture with a 3D porous structure and high porosity, wrinkled sheetlike structure with rich edges. These typical structures identify that graphene has been prepared successfully *via* laser-scribing a PI matrix. After the laser patterning procedure, NiCo-LDH was electrodeposited on the LIG sheets. As displayed in the SEM and TEM images (Fig. 2C, D), the NiCo-LDH nanoflakes are highly-dense, uniformly distributed along the LIG skeleton without any evident damage or alteration of the initial 3D porous structure of LIG, which is expected to enlarge the surface area, offer more active sites and high electrocatalytic activity toward Glu oxidation.

Additionally, the EDS elemental mapping of NiCo-LDH/LIG composites (Fig. 2E and F) confirm that the NiCo-LDH/LIG composites are composed of C, Ni, Co and O elements. All elements evenly distribute over the surface and interface of NiCo-LDH/LIG, implying the uniform composition of NiCo-LDH onto the LIG surface. By merging the advantages of a three-dimensional (3D) porous architecture of LIG foam with NiCo-LDH nanoflakes including rapid electron transfer, numerous active sites and excellent electrocatalytic ability toward Glu, the developed NiCo-LDH/LIG electrode will show excellent electrochemical activity for sensing Glu.

The XRD tests were used to investigate the crystallographic structure and purity of LIG and NiCo-LDH/LIG samples. In the XRD profiles of LIG and NiCo-LDH/LIG

samples (Fig. 3A), a broad diffraction signal is centered at  $26.0^\circ$ . It can be assigned to (002) facet of graphene, identifying that graphene was gained by transforming PI by patterned laser irradiation. Compared with LIG, NiCo-LDH/LIG samples have four new diffraction peaks detected at  $11.6^\circ$ ,  $23.3^\circ$ ,  $34.9^\circ$ , and  $60.9^\circ$ , corresponding to the NiCo-LDH (003), (006), (012), and (110) planes (JCPDS 33-0429), respectively [26]. These results indicate that the successful formation of NiCo-LDH/LIG composite without other impurities was accomplished in this work.

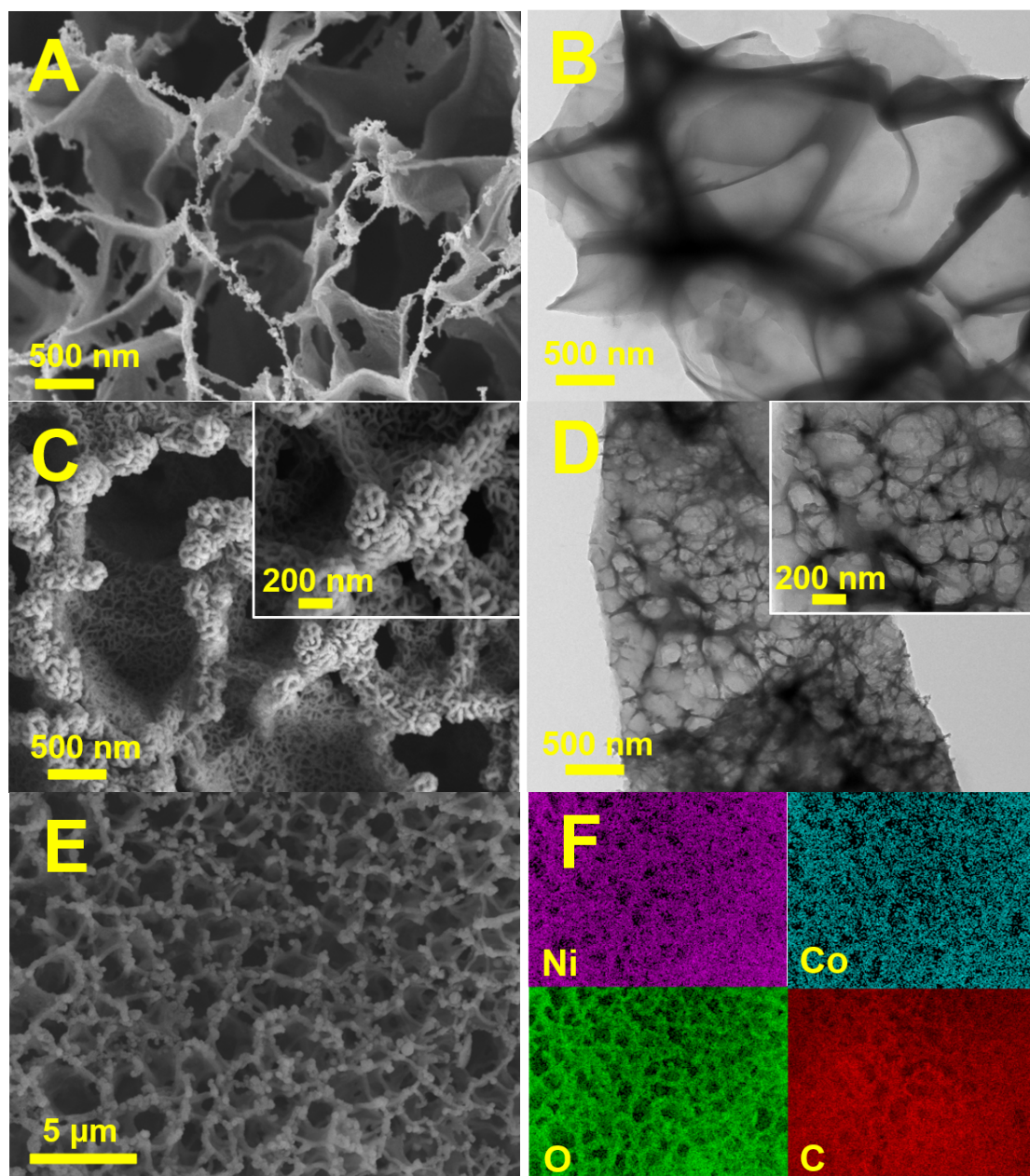


**Figure 2.** SEM (A,C) and TEM (B,D) images of LIG (A,B), NiCo-LDH/LIG (C,D) and corresponding element distribution (E,F) of NiCo-LDH/LIG composites.

In order to prove the existence of multilayer graphene, Raman characterization

was performed on the LIG and NiCo-LDH/LIG samples (Fig. 3B). Obviously, the Raman spectra reveal three characteristic peaks of graphene-derived materials, involving the D band at  $\sim 1350\text{ cm}^{-1}$ , the G band at  $\sim 1580\text{ cm}^{-1}$  and the 2D band at  $\sim 2700\text{ cm}^{-1}$ . All of them confirm the formation of graphene in LIG and NiCo-LDH/LIG samples. Moreover, the average ratio of 2D/G peak intensity is 0.576 and 0.594 for LIG and NiCo-LDH/LIG, respectively, suggesting the formation of multilayer graphene [33].

The XPS characterization was conducted on NiCo-LDH/LIG samples to clarify their chemical environment and valence states. For the NiCo-LDH/LIG samples (Figure 3C), the typical C 1s, O 1s, Co 2p and Ni 2p peaks are obviously observed, revealing the presence of nickel, carbon, oxygen and cobalt elements. The specific information was then obtained from the deconvoluted spectrum of Co 2p and Ni 2p. In the Co 2p high-resolution spectrum (Fig. 3D), there are two diffusive broad peaks of Co  $2p_{3/2}$  and Co  $2p_{1/2}$  peaks located at 781.6 eV and 797.1 eV, which can be further deconvoluted into a couple of peaks and two satellites (labelled as Sat.) at 787.8 and 803.8 eV. One couple of peaks at 781.6 and 796.9 eV may attribute to  $\text{Co}^{3+}2p_{3/2}$  and  $\text{Co}^{3+}2p_{1/2}$ , and the other couple at 783.3 and 798.3 eV attribute to  $\text{Co}^{2+}2p_{3/2}$  and  $\text{Co}^{2+}2p_{1/2}$ , which confirm the presence of  $\text{Co}^{3+}$  and  $\text{Co}^{2+}$  in NiCo-LDH/LIG samples [26]. Moreover, the high-resolution spectrum of Ni2p (Fig. 3E) shows two pairs according with  $\text{Ni}^{2+}$  (856.5/874.2 eV) and two satellites at 862.4 and 880.4 eV [26]. All these results confirmed the effective preparation of NiCo-LDH on the LIG surface.

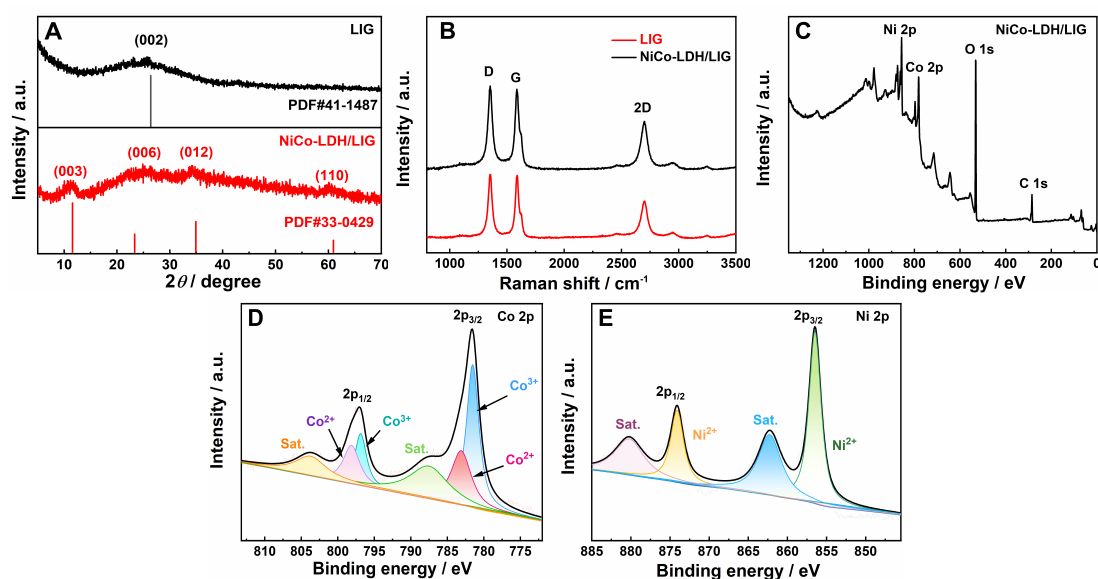


**Figure 3.** XRD spectra (A) and Raman spectra (B) of LIG and NiCo-LDH/LIG; Full

XPS spectra (C) of NiCo-LDH/LIG, and the corresponding deconvoluted spectra of Co 2p(D), Ni 2p(E) in NiCo-LDH/LIG.

### 3.2. Electrochemical performance study of NiCo-LDH/LIG

Electrochemical tests were performed to explore the electron transfer capabilities of LIG, NiCo-LDH/LIG, GCE and NiCo-LDH/GCE in a 0.1 M KCl aqueous electrolyte containing 5.0 mM  $[\text{Fe}(\text{CN})_6]^{3-/4-}$  at a scanning range of 5 mV s<sup>-1</sup> (Fig. 4 A). The anodic peak current of a bare GCE is 37.57  $\mu\text{A}$ . After the modification of NiCo-LDH on a GCE, the anodic peak current is reduced to 20.49  $\mu\text{A}$  because of the low electronic conductivity of NiCo-LDH, impeding the electron transfer approach on the NiCo-LDH/GCE surface. Compared with a GCE, the anodic peak current increases to 53.25  $\mu\text{A}$  when using the LIG as the working electrode owing to the improved electron transfer triggered by the high electrical conductivity of LIG. Similarly, due to the low electronic conductivity of NiCo-LDH, the anodic peak current of 48.67  $\mu\text{A}$  is gained on a NiCo-LDH/LIG electrode.

In addition, EIS measurements were carried out to examine the electron transport kinetics of LIG, NiCo-LDH/LIG, GCE and NiCo-LDH/GCE. The Nyquist plots of LIG, NiCo-LDH/LIG, GCE and NiCo-LDH/GCE were recorded in a 0.1 M KCl aqueous electrolyte plus 5.0 mM  $[\text{Fe}(\text{CN})_6]^{3-/4-}$  at open circuit potentials. (Fig. 4B). Inside them, the semicircle at a higher frequency region represents the charge transfer resistance ( $R_{ct}$ ). A Randles circuit (the inset in Fig. 4B) was further utilized to fit these Nyquist plots. The model consists of the double-layer capacitance ( $C_{dl}$ ), the electrolyte resistance ( $R_s$ ), Warburg impedance ( $Z_w$ ) and  $R_{ct}$ , of which the values are shown in Table 1.

The GCE has the  $R_{ct}$  value of about 176.4  $\Omega$ . An obvious increase of  $R_{ct}$  value (1394.8  $\Omega$ ) was observed when NiCo-LDH was modified on GCE, suggesting the poor electrical conductivity of NiCo-LDH. Compared with the GCE, the Nyquist curve of LIG presents a reduction for the  $R_{ct}$  value (51.3  $\Omega$ ), signifying the decreased electron transfer resistance and the improved electrical conductivity for the LIG to the GCE. The NiCo-LDH/LIG owns an  $R_{ct}$  of about 68.8  $\Omega$  since NiCo-LDH renders the electron transport between the probe and electrode more difficult.

The electrocatalytic behavior of LIG, NiCo-LDH/LIG, GCE and NiCo-LDH/GCE toward the oxidation of Glu was examined in 0.1 M NaOH solution with Glu-free (dashed line) and 2 mM Glu (solid line) at a scanning range of 5 mV s<sup>-1</sup>. From the cyclic voltammetric (CV) responses (Fig. 4C), It can be observed that the

CV response of either a bare LIG or a bare GCE does not vary notably before and after the injection of 2 mM Glu, suggesting no catalytic activity of these electrodes toward Glu. However, one couple of broad redox peaks appears in the presence of Glu (solid line) when NiCo-LDH/LIG and NiCo-LDH/GCE are used as the working electrode, which are generated by overlapped redox peaks of Ni(II)/Ni(III) and Co(II)/Co(III) in an alkaline electrolyte. After 2 mM Glu is dropped into the electrolyte, a significant increase of the signal is seen, suggesting that NiCo-LDH possesses a high electrocatalytic ability toward Glu oxidation. Notably, compared with the increased current intensity on NiCo-LDH/GCE, a larger improvement of response current is observed on NiCo-LDH/LIG, which can be attributed to the inferior electrochemical capability of a GCE, indicating the excellent electron transfer capability and a large electrochemical active surface area of LIG.

In order to further study the electrocatalyst's activity, the electrochemical surface areas (ESCA) of LIG, NiCo-LDH/LIG, GCE and NiCo-LDH/GCE were estimated by determining their double-layer capacitances ( $C_{dl}$ ) since ESCA is proportional to  $C_{dl}$  [7]. To estimate  $C_{dl}$  values, the CV plots of LIG, NiCo-LDH/LIG, GCE and NiCo-LDH/GCE were obtained at varying scan rates (75 - 175  $\text{mV s}^{-1}$ ) in the non-faradic region from 0 to 0.2 V (Fig. 4D-4G). From the calibration curve of the current density ( $\Delta j$ ) at 0.10 V versus sweep speeds, the calculated  $C_{dl}$  values of GCE, NiCo-LDH/GCE, LIG and NiCo-LDH/LIG are 117.10, 46.22, 1220.00 and 5200.00  $\mu\text{F cm}^{-2}$ , respectively (Fig. 4H). Consequently, the NiCo-LDH/LIG acquires the largest ECSA value, demonstrating more catalytic active sites and thereby significantly simplifying the Glu adsorption.

On the basis of the above outcomes, the excellent sensing capability of the NiCo-LDH/LIG electrode for Glu is expected, probably originated from the cooperative effect of NiCo-LDH and LIG. The porous graphene network endows an enlarged electrochemical surface area, accelerates the charge transport kinetics and also functions as a perfect substrate for NiCo-LDH nanoflakes deposition. The homogenous distribution of high dense NiCo-LDH nanoflakes on LIG offers supplementary exposed active sites and enhances the catalytic activity towards Glu oxidation, and LIG accelerates the electron transference.

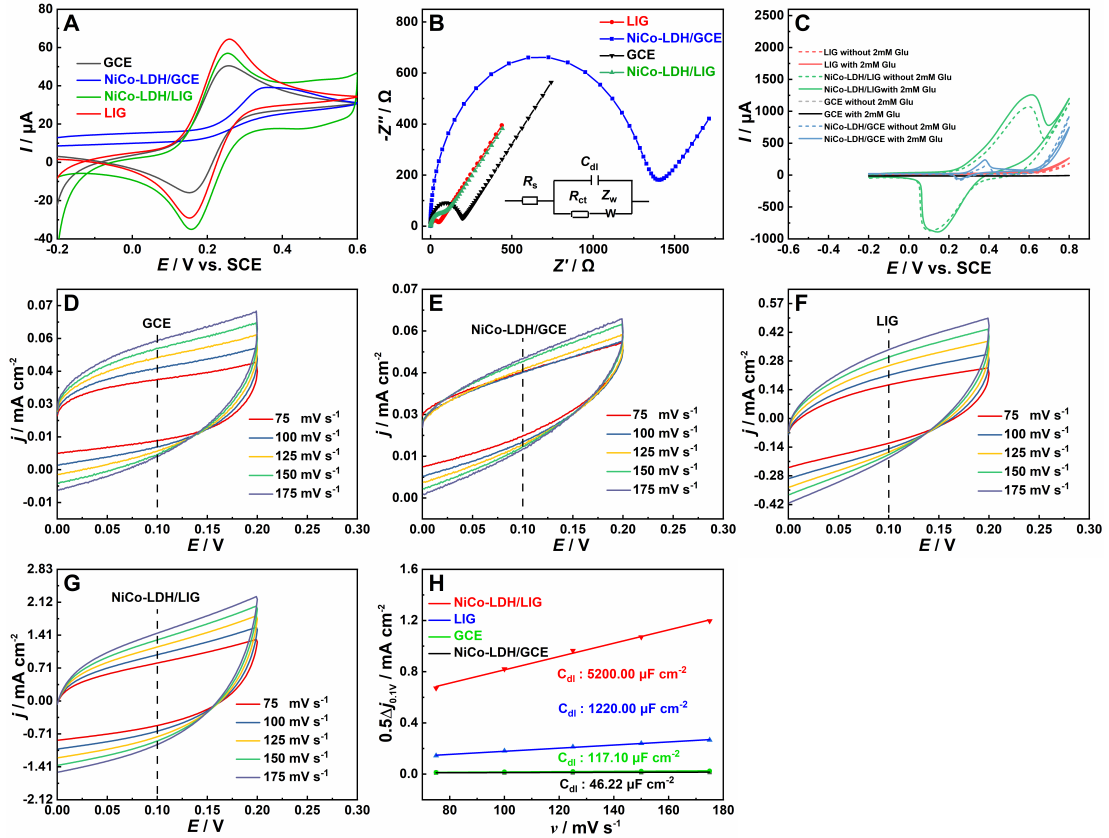


**Figure 4.** CVs (A) and EIS spectra (B) of LIG, NiCo-LDH/LIG, GCE and NiCo-LDH/GCE in 0.1 M KCl containing an equimolar (5 mM) mixture of  $K_3Fe(CN)_6$  and  $K_4Fe(CN)_6$ . Inset in (B): Randle's circuit model. (C) CVs of LIG, NiCo-LDH/LIG, GCE and NiCo-LDH/GCE in 0.1 M NaOH with Glu-free (dashed line) and 2 mM Glu (solid line) at  $10 \text{ mV s}^{-1}$ . (D-G) CVs of various electrodes in 2 M KCl at different sweep speeds in non-Faraday potential regions. (H) Calibration plots of  $\Delta j = j_a - j_c$  at 0.10 V vs. different sweep speeds.

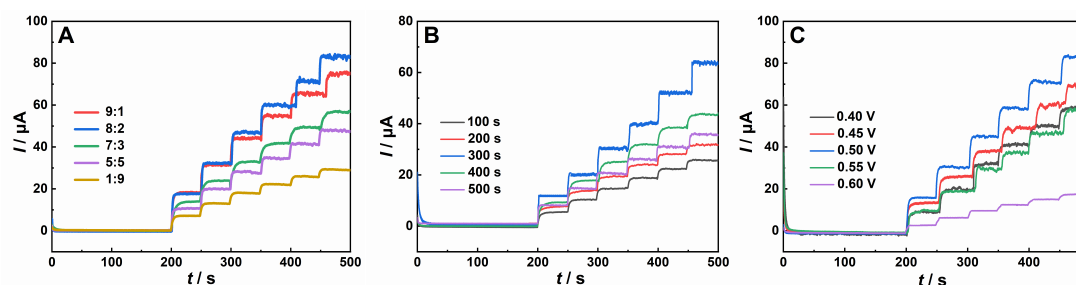
**Table 1.** The electrochemical impedance data of LIG, NiCo-LDH/LIG, GCE and NiCo-LDH/GCE in 5 mM  $[Fe(CN)_6]^{3-/4-}$  + 0.1 M KCl.

Electrode	$R_s(\Omega)$	$C_{dl}(F)$	$R_{ct}(\Omega)$	$Z_w(\Omega \text{ s}^{-1/2})$
LIG	287.3	$0.219 \times 10^{-5}$	51.3	0.0021
NiCo-LDH/LIG	198.5	$3.950 \times 10^{-5}$	68.8	0.0023
GCE	87.8	$0.054 \times 10^{-5}$	176.4	0.0014
NiCo-LDH/GCE	111.8	$0.055 \times 10^{-5}$	1394.8	0.00069

### 3.3. Electrochemical detection of Glu

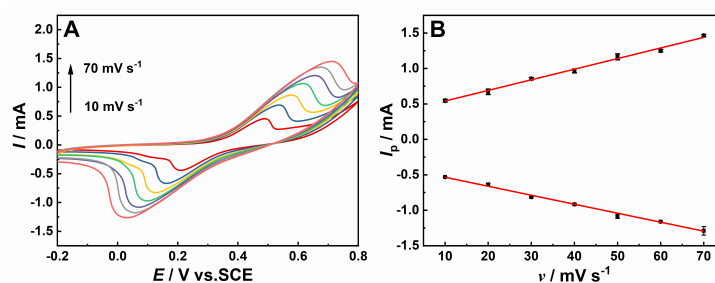
To achieve the best performance of the determination sensitivity of NiCo-LDH/LIG toward Glu, the ratio of Ni and Co in NiCo-LDH, the electrodeposition time of NiCo-LDH and the applied potential were optimized. The influence of Ni:Co

mole ratios toward Glu detection by NiCo-LDH/LIG was explored (Fig. 5A). With an increase of a Ni:Co molar ratio from 1:9 to 8:2, the current signal strengthens. However, it declines when the Ni:Co molar ratio exceeds 8:2. The response current for Glu displays a tendency of a gradual growth with the prolonging of electrodeposition time from 100 s to 300 s and exhibits lower values when the deposition time is higher than 300 s (Fig. 5B). Moreover, the influence of different applied potentials (0.40-0.60 V) on the current density of NiCo-LDH/LIG was studied (Fig. 5C). The modified electrode delivers a maximum current signal at the working potential of 0.50 V. Therefore, a Ni:Co molar ratio of 8:2, an optimal deposition of 300 s, and an applied potential of 0.50 V were applied for the subsequent experiments.



**Figure 5.** Effect of the Ni:Co molar ratio (A) and deposition time (B) for the production of NiCo-LDH on the LIG surface as well as applied detection potential (C) on the Glu current response.

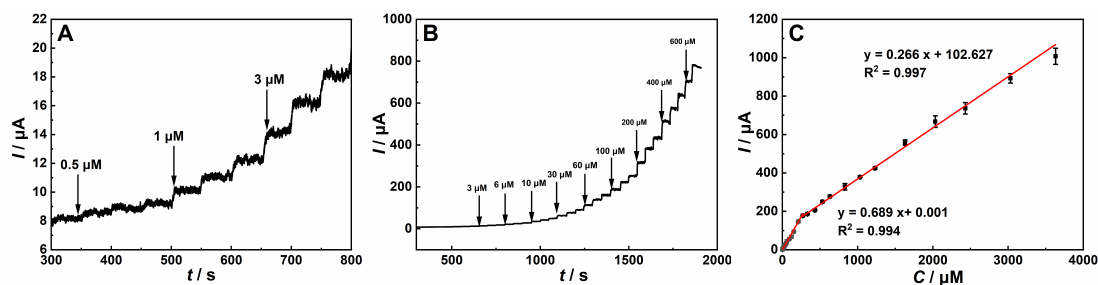
To study the mass transport process on the NiCo-LDH/LIG, its CVs were recorded upon adding 2 mM Glu (Fig. 6A) at varied scan rates ( $\nu$ ) ranging from 10 to 70  $\text{mV s}^{-1}$ . It can be noticed that both the anodic and cathodic peak currents ( $I_{\text{pa}}$  and  $I_{\text{pc}}$ ) progressively increase with an increase of scan rate ( $\nu$ ). Moreover, the  $I_{\text{p}}$  (i.e.,  $I_{\text{pa}}$  and  $I_{\text{pc}}$ ) has a linear correlation with  $\nu$ , suggesting that the electron transfer at the NiCo-LDH/LIG electrode is an adsorption-controlled process (Fig. 6B).



**Figure 6.** (A) CVs of a NiCo-LDH/LIG sensor at varied scan rates of 10 - 70  $\text{mV s}^{-1}$  in 0.1 M NaOH + 2 mM Glu. (B) The relationship between  $I_{\text{p}}$  ( $I_{\text{pa}}$  and  $I_{\text{pc}}$ ) and the scan

rate ( $v$ ).

Due to the great electrooxidation activity of NiCo-LDH/LIG towards Glu, a NiCo-LDH/LIG sensor for amperometric quantitation of Glu was successfully developed. In the recorded amperometric current-time ( $i-t$ ) response of NiCo-LDH/LIG by consecutively injecting different levels of Glu under the optimal detection conditions (Fig. 7A and 7B establish), one can notice that there is a fast current response and then a stable state after the injection of Glu, which prove that NiCo-LDH/LIG possesses an outstanding activity for Glu sensing. Furthermore, the amperometric signals possess positive linear relationships (Fig. 7C) with the level of Glu from 0.5 to 270  $\mu\text{M}$  and from 0.27 to 3.6 mM. Their linear regression equations can be expressed as  $y$  ( $\mu\text{A}$ ) =  $0.689x$  ( $\mu\text{M}$ ) + 0.001 ( $R^2 = 0.994$ ) and  $y$  ( $\mu\text{A}$ ) =  $0.266x$  ( $\mu\text{M}$ ) + 102.627 ( $R^2 = 0.997$ ), with their corresponding sensitivities of  $9.750 \mu\text{A} \mu\text{M}^{-1} \text{cm}^{-2}$  and  $3.760 \mu\text{A} \mu\text{M}^{-1} \text{cm}^{-2}$ , respectively. The limit of detection (LOD) was estimated to be 0.05  $\mu\text{M}$  with an error limit of 1.4% according to the formula  $3\sigma/S$ . Besides, the response time of NiCo-LDH/LIG in Glu determination is recorded at 2 s (Fig. 7D). The electrochemical signal only declines just 6.78% even after running for 200 s (Fig. 7E). Electrochemical sensing performance of a NiCo-LDH/LIG-based sensor is compared with other recently reported Glu sensors (Table 2), demonstrating that the NiCo-LDH/LIG-based sensor displays superior properties. Essentially, the prominent catalytic effect of the NiCo-LDH and the high electron conductivity and large electroactive surface area of LIG may account for the extraordinary electrocatalytic activity for Glu sensing in the NiCo-LDH/LIG-based sensor. Therefore, it seems hopeful for the future of NiCo-LDH/LIG in the construction of electrochemical Glu sensing platform that does not depend on enzymes.



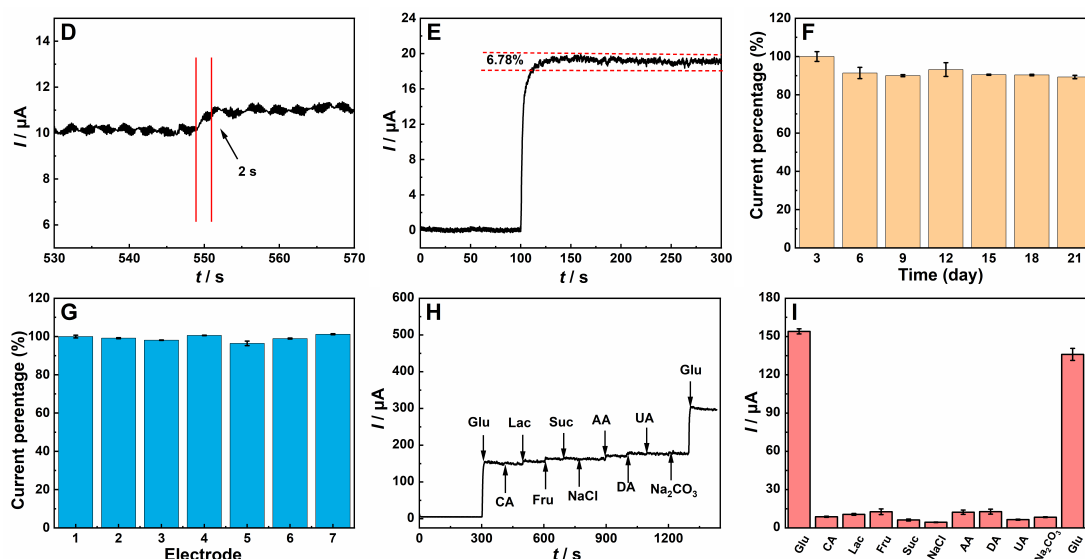


**Figure 7.** (A,B) Chronoamperometric responses of the NiCo-LDH/LIG with increasing Glu concentration at 0.50 V. (C) The calibration curve of Glu concentration vs. amperometric signals. (D) Response time of NiCo-LDH/LIG electrode. (E) Amperometric response of NiCo-LDH/LIG by adding Glu in 0.1 M NaOH. (F) long-term stability of NiCo-LDH/LIG every 3 days. (G) Reproducibility of seven randomly selected NiCo-LDH/LIG-based Glu sensors. (H) The amperometric *i-t* response on the NiCo-LDH/LIG electrode by the sequential addition of 1.0 mM Glu and 1.0 mM different potentially interfering substances. (I) The bar graph of comparison of the current signals with Glu and potentially interfering substances.

**Table 2.** Performance comparison of the NiCo-LDH/LIG sensor with other Glu sensors.

Electrode	Sensitivity ( $\mu\text{A } \mu\text{M}^{-1} \text{ cm}^{-2}$ )	Linear range ( $\mu\text{M}$ )	LOD ( $\mu\text{M}$ )	Ref.
Cu <sub>2</sub> O/MXenes/activated carbon	0.430	4-28400	1.96	[39]
MnCO <sub>3</sub> /LIG/GCE	2.731	5-55	2.2	[40]
GS/NPG/PANI/Fe <sub>3</sub> O <sub>4</sub> @MIL-101-NH <sub>2</sub>	61.183	0.5-25000	0.3	[41]
CoO nanowire/Ni foam	28.22	5-2525	0.5	[42]
MIL-88A@Ni <sub>10</sub> Fe Prussian Blue-50	1.963	5-1000	0.12	[43]

Zn-MOF/MWCNTs	0.034	20-8140	3.7	[44]
NiCo/macroporous carbon/GCE	0.206	0.1-831.7	0.06 3	[45]
CuCoP@Cu(OH) <sub>2</sub> /GCE	8.351	1-2530	2.3	[46]
Au/CuO/SPCE	0.237	2-397	7.24	[47]
NiCu-MOF/GCE	1.832	20-4930	15	[48]
Cu-MOF/PtNPs/GE	0.158	400-25000	60	[49]
CuCo-MOF/CC	0.868	0.25-2374	0.27	[50]
Ni/Co(HHTP)MOF/CC	3.250	0.3-2312	0.1	[51]
Fe <sub>x</sub> Co <sub>y</sub> O <sub>4</sub> -rGO/SPCE	1.510	0.1-1906	0.07	[52]
NiCo-LDH/LIG	9.750	0.5-270	0.05	This
	3.760	270-3600		work

GCE: glassy carbon electrode; CC: carbon cloth; GE: gold electrode; SPCE: screen-printed carbon electrode; GS/NPG/PANI: graphite sheet/ nitrogen-doped functionalized graphene/polyaniline.

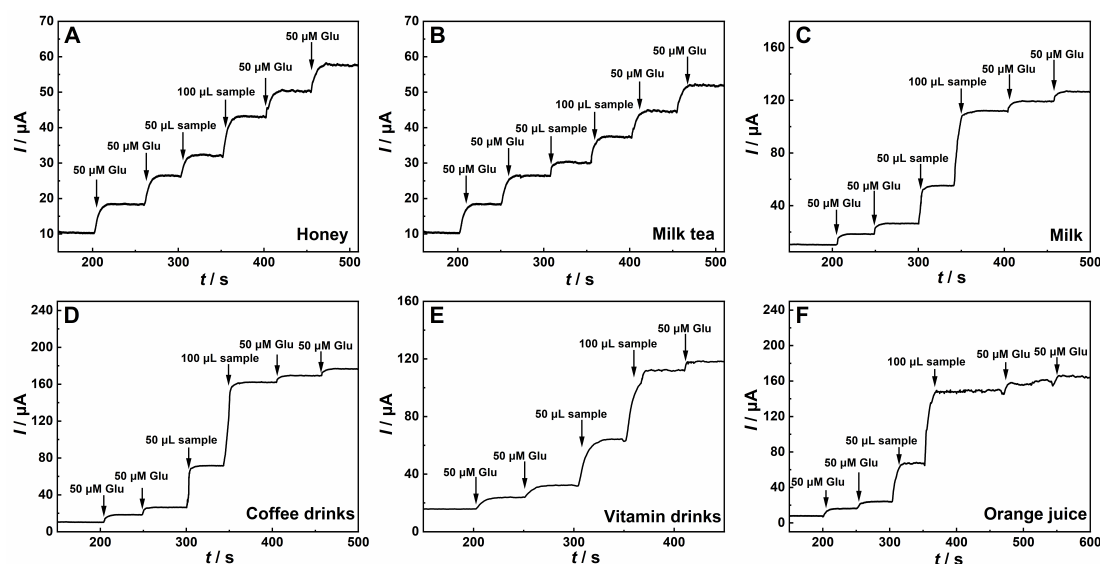
Several key attributes of the constructed Glu sensor have been evaluated, including its reproducibility, specificity, stability and repeatability. The long-term stability of a NiCo-LDH/LIG-based sensor was assessed by determining the response current value of 1 mM Glu at 0.50 V in 0.1 M NaOH. The electrochemical signals showed the outstanding stability with a reduction of 6.8% during the 21-day experiment (Fig. 7F). Thus, the NiCo-LDH/LIG-based sensor owns a preferable stability for Glu sensing. Meanwhile, seven independent NiCo-LDH/LIG electrodes were used to determine the electrochemical signals of 50  $\mu$ M Glu under the same conditions. It has been found that the NiCo-LDH/LIG electrodes offered the relative standard deviation (RSD) of as low as of 1.6 %, indicating a reliable reproducibility of the NiCo-LDH/LIG electrodes. The repeatability of the same NiCo-LDH/LIG electrode was surveyed through determining 50  $\mu$ M Glu for seven times constantly. The obtained RSD was 2.8% and it supplied a powerful proof that the NiCo-LDH/LIG-based sensor exhibits an acceptable repeatability (Fig. 7G).

One of the challenges in non-enzymatic Glu sensor is the electrochemical signal changes triggered by potentially interfering substances. In our case (Fig. 7H), 1 mM Glu and 1 mM various interfering substances including citric acid (CA), lactose (Lac), uric acid (UA), sucrose (Suc), ascorbic acid (AA), fructose (Fru), NaCl, dopamine

(DA), and  $\text{Na}_2\text{CO}_3$  have been continuously added into 0.1 M NaOH solution, followed by the final injection of 1 mM Glu. There are no obvious electrochemical signal variations after the injection of 1 mM other species. Meanwhile, the current response of Glu is almost constant after adding other interferents (Fig. 7I). Thus, the NiCo-LDH/LIG sensing platform possesses remarkable selectivity for Glu sensing to resist the interferences.

To assess the feasibility of the proposed NiCo-LDH/LIG sensor towards the Glu detection, a series of samples including coffee drinks, milk, milk tea, cola, orange juice, vitamin drinks, honey and human serum were selected as the actual samples. The amperometric response was recorded for successive additions of Glu standard solution, varying quantities of the actual samples, and standard Glu solution into 0.1 M NaOH (Fig. 8). The real Glu content in these food and human serum samples was then determined and compared with that measured by means of the UV-Vis spectrophotometry (Table 3). There was no significant difference of the determined consequences, ratifying the excellent practicability of established Glu sensing platform. Moreover, the spiking and recovery experiment was carried out using the prepared sensor and the UV-Vis spectrophotometry. The results and the acceptable recovery rates (ranged from 96.3 % to 102.0 %) demonstrate that the established electrochemical sensing platform provides a reliable and precise approach for Glu determination in real food and human serum.

### 3.4. Practical applications



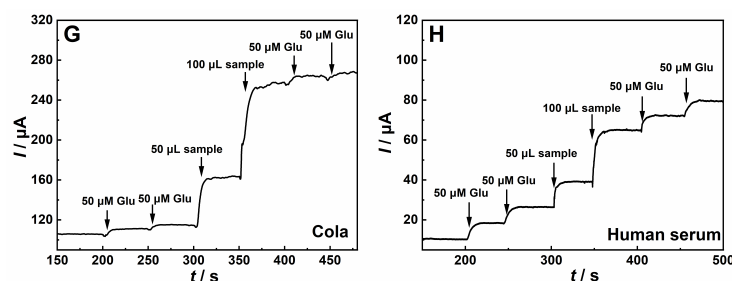


**Figure 8.** Amperometric response of a NiCo-LDH/LIG toward sequential addition of 50  $\mu\text{M}$  Glu, 50  $\mu\text{L}$ , and 100  $\mu\text{L}$  various samples including honey (A), milk tea (B), milk (C), coffee drinks (D), vitamin drinks (E), orange juice (F), cola (G), and human serum (H), followed by injecting 50  $\mu\text{M}$  Glu.

#### 4. Conclusions

In summary, a laser-induced technique was used to prepare a porous laser-induced graphene (LIG) electrode, on which high dense NiCo-LDH nanoflakes were electrodeposited. This NiCo-LDH/LIG electrode was then utilized for non-enzymatic glucose (Glu) sensing. It displays superior sensing performance toward Glu, mostly profiting from the cooperative effect of NiCo-LDH and LIG. The NiCo-LDH/LIG sensors maintained long-term stability, reproducibility and high selectivity for Glu sensing. Moreover, the NiCo-LDH/LIG sensors can be utilized for the detection of Glu in food samples and human serum with reliable accuracy, indicating the potential practical application. In a nutshell, the NiCo-LDH/LIG electrodes can provide a way of developing nonenzymatic electrochemical sensors to analyze the Glu in human serum and food samples.

**Table 3.** The measurement values of Glu through UV-Vis spectrophotometer and NiCo-LDH/LIG electrode in food and human serum samples.

Sample	Added (mM)	NiCo-LDH/LIG			By UV-Vis		
		Detected (mM)	Recovery (%)	RSD (%)	Detected (mM)	Recovery (%)	RSD (%)
Coffee drinks	0	13.00	-	-	13.06	-	1.6
	50	60.36	96.0	0.6	61.52	97.6	2.7
	75	85.32	97.0	0.9	86.78	98.5	1.3
Milk	0	8.37	-	-	8.73	-	0.4
	50	57.36	98.3	0.1	58.07	99.0	0.2
	75	85.02	102.0	1.0	81.35	97.2	0.1
Milk tea	0	1.18	-	-	1.18	-	1.8

	50	51.05	99.7	0.5	50.92	99.5	4.1
	75	75.21	98.7	2.5	74.57	97.9	4.0
Cola	0	29.49	-	-	29.11	-	3.8
	50	79.87	100.5	0.4	78.59	99.4	3.2
	75	100.58	96.3	1.9	103.51	99.4	4.4
Orange juice	0	17.37	-	-	17.38	-	4.4
	50	67.48	100.2	1.2	66.51	98.7	3.3
	75	90.25	97.7	1.7	89.71	97.1	3.0
Vitamin drinks	0	11.87	-	-	11.86	-	2.3
	50	61.58	99.5	2.0	60.66	98.1	0.1
	75	86.21	99.2	2.5	85.32	98.2	1.1
Honey	0	1.410	-	-	1.43	-	0.1
	50	50.35	98.0	0.5	51.00	99.2	3.7
	75	76.17	99.7	0.7	75.58	98.9	2.8
Human serum	0	3.53	-	-	3.50	-	0.9
	50	53.25	99.5	0.3	51.89	97.0	3.3
	75	77.24	98.4	0.6	76.35	97.3	4.3

### Declaration of competing interest

The authors declare that they have no known competing financial interests or relevant relationships that could have appeared to influence the work reported in this paper.

### Data availability

Data will be made available on request.

### Acknowledgements

This work was financially supported by open project funding of Ministry of Education Key Laboratory for the Synthesis and Application of Organic Functional Molecules of Hubei University of China (No. KLSAOFM2302), the Natural Science Foundation of Hubei Province of China (No. 2021CFB1192) and the Graduate Innovative Fund of Wuhan Institute of Technology of China. Thanks to eceshi ([www.eceshi.com](http://www.eceshi.com)) for the XRD analysis.

### References

- [1] M. Tan, M. Ni, X. Liu, B. Qu, X. Lin, D. Jiang, Y. Yuan, H. Du, Surface adsorption guided design of semicrystalline nickel-iron hydroxide for highly-sensitive glucose sensing, *Chem. Eng. J.* 451 (2023) 138963.
- [2] L. He, J. Su, T. You, S. Xiao, P. Huang, D. He, P. Jiang, Rapid and facile

- preparation of NiFe-layered double hydroxide nanosheets as self-supported electrode for glucose detection in drink sample, *Food Chem.* 439 (2024) 138163.
- [3] Y. Chen, Q. Yao, L. Zhang, P. Zeng, HPLC for simultaneous quantification of free mannose and glucose concentrations in serum: use in detection of ovarian cancer, *Front. Chem.* 11 (2023) 1289211.
- [4] J. Xu, X. Jian, J. Guo, J. Zhao, J. Tang, Y. Zhao, J. Xu, Z. Gao, Y.-Y. Song, Selective SERS identification and quantification of glucose enantiomers on homochiral MOFs based enzyme-free nanoreactors, *Chem. Eng. J.* 459 (2023) 141650.
- [5] N. Wen, J. Li, W. Zhang, P. Li, X. Yin, W. Zhang, H. Wang, B. Tang, Monitoring the progression of early atherosclerosis using a fluorescence nanoprobe for the detection and imaging of phosphorylation and glucose levels, *Angew. Chem. Int. Ed.* 62 (2023) e202302161.
- [6] C. Zhang, C. Wei, D. Chen, Z. Xu, X. Huang, Construction of inorganic-organic cascade enzymes biosensor based on gradient polysulfone hollow fiber membrane for glucose detection. *Sensor. Actuat. B-Chem.* 385 (2023) 133630.
- [7] P. Liu, Y. Zhang, L. Ye, M. Huang, T. Zeng, J. Yang, F. Tian, Z. Wu, X. Zhang, C. Hu, N. Yang, Laser-induced graphene decorated with Ni-Pt alloy nanoparticles for non-enzymatic electrochemical quantification of glucose, *Diam. Relat. Mater.* 146 (2024) 111205.
- [8] X. Tang, X. Yuan, Y. Jin, J. Wu, C. Ling, K. Huang, L. Zhu, X. Xiong, A novel hollow CuMn-PBA@NiCo-LDH nanobox for efficient detection of glucose in food, *Food Chem.* 438 (2024) 137969.
- [9] Y. Zou, Z. Chu, J. Guo, S. Liu, X. Ma, J. Guo, Minimally invasive electrochemical continuous glucose monitoring sensors: Recent progress and perspective, *Biosens. Bioelectron.* 225 (2023) 115103.
- [10] Y. Pan, M. He, J. Wu, H. Qi, Y. Cheng, One-step synthesis of MXene-functionalized PEDOT: PSS conductive polymer hydrogels for wearable and noninvasive monitoring of sweat glucose, *Sensor. Actuat. B-Chem.* 401 (2024) 135055.
- [11] S. Gengan, R.M. Gnanamuthu, S. Sankaranarayanan, V.M. Reddy, B.C. Marepally, R.K. Biroju, Electrochemical modified Pt nanoflower@rGO for non-enzymatic electrochemical sensing of glucose, *Sensor. Actuat. A-Phys.* 353 (2023) 114232.

- [12] F.J. Rahmania, T. Imae, J.P. Chu, Electrochemical nonenzymatic glucose sensors catalyzed by Au nanoclusters on metallic nanotube arrays and polypyrrole nanowires, *J. Colloid Interf. Sci.* 657 (2024) 567-579.
- [13] C. He, M. Asif, Q. Liu, F. Xiao, H. Liu, B.Y. Xia, Noble metal construction for electrochemical nonenzymatic glucose detection, *Adv. Mater. Technol.* 8 (2023) 2200272.
- [14] G. Li, C. Wang, Y. Chen, F. Liu, H. Fan, B. Yao, J. Hao, Y. Yu, D. Wen, Dual structural design of platinum-nickel hydrogels for wearable glucose biosensing with ultrahigh stability, *Small* 19 (2023) 2206868.
- [15] J. Wu, X. Tang, S. Zhao, Y. Zhang, C. Ling, Y. Xing, H. Yu, K. Huang, Z. Zou, X. Xiong, Microplasma and quenching-induced Co doped NiMoO<sub>4</sub> nanorods with oxygen vacancies for electrochemical determination of glucose in food and serum, *Food Chem.* 414 (2023) 135755.
- [16] H. Yin, X. Bai, Z. Yang, Activating Ni nanoparticles into Ni single atoms by N doping for high-performance electrochemical sensing of glucose, *Chem. Eng. J.* 478 (2023) 147510.
- [17] Y. Zhang, Y. Huang, P. Gao, W. Yin, M. Yin, H. Pu, Q. Sun, X. Liang, H.-b. Fa, Bimetal-organic frameworks MnCo-MOF-74 derived Co/MnO@HC for the construction of a novel enzyme-free glucose sensor, *Microchem. J.* 175 (2022) 107097.
- [18] Z. Shao, Q. Gao, S. Sun, L. Wu, W. Feng, MOF-derived CuO/CNT for high sensitivity and fast response glucose sensing, *Sensor. Actuat. B-Chem.* 398 (2023) 134713.
- [19] C. Shamili, A.S. Pillai, S. S, A. Chandra, M.R. Varma, S.K. Peethambharan, All-printed wearable biosensor based on MWCNT-iron oxide nanocomposite ink for physiological level detection of glucose in human sweat, *Biosens. Bioelectron.* 258 (2024) 116358.
- [20] Y. Yang, R. Jiang, M. Wang, J. Xiong, Y. Cheng, H. Zhang, L. Chen, 3D gyrosopic copper-based metal-organic framework for high sensitivity detection of glucose and H<sub>2</sub>O<sub>2</sub>, *Microchem. J.* 200 (2024) 110224.
- [21] Y. Shu, Z. Shang, T. Su, S. Zhang, Q. Lu, Q. Xu, X. Hu, A highly flexible Ni-Co MOF nanosheet coated Au/PDMS film based wearable electrochemical sensor for continuous human sweat glucose monitoring, *Analyst* 147 (2022) 1440-1448.
- [22] M. Liu, T. Gao, H. Li, B. Xie, C. Hu, Y. Guo, Dan Xiao, Preparation of

- amorphous Ni/Co bimetallic nanoparticles to enhance the electrochemical sensing of glucose, *Microchem. J.* 191 (2023) 108731.
- [23] C.-T. Lo, Y.-S. Wu, S.-M. Huang, P.-J. Tsai, C.-L. Lee, Carbon fibre-supported hierarchical NiCo layered double hydroxide nanosheets as non-enzymatic glucose sensors for sport drinks and serum, *Food Chem.* 383 (2022) 132383.
- [24] M. Yuan, Z. He, L. Tan, Z. Liao, Y. Liu, Y. Zhang, X. Xiong, In situ preparation of hierarchical CuO@NiCo LDH core-shell nanosheet arrays on Cu foam for highly sensitive electrochemical glucose sensing. *New J. Chem.* 47 (2023) 21446-21453.
- [25] M. Abdelkadir, A.-A. Leila, Fabrication of hierarchical Ni nanowires@NiCo-layered double hydroxide nanosheets core-shell hybrid arrays for high-performance hybrid supercapacitors, *Electrochim. Acta* 439 (2023) 141622.
- [26] Y. Zhu, J. Qian, K. Xu, W. Ouyang, J. Yang, N. Yang, Hollow nanocages heterostructured NiCo-LDH/MWCNTs electrocatalyst for highly sensitive and non-invasive detection of saliva glucose, *Chem. Eng. J.* 485 (2024) 149795.
- [27] F. Sun, X. Wang, Z. You, H. Xia, S. Wang, C. Jia, Y. Zhou, J. Zhang, Sandwich structure confined gold as highly sensitive and stable electrochemical non-enzymatic glucose sensor with low oxidation potential, *J. Mater. Sci. Technol.* 123 (2022) 113-122.
- [28] M. Cao, Y. Zou, Y. Zhang, T. Zeng, Q. Wan, G. Lai, N. Yang, Robust and selective electrochemical sensing of hazardous photographic developing agents using a MOF-derived 3D porous flower-like Co<sub>3</sub>O<sub>4</sub>@C/graphene nanoplate composite, *Electrochim. Acta* 409 (2022) 139967.
- [29] C. Guo, Y. Zhang, T. Zeng, D. Huang, Q. Wan, N. Yang, High-performance asymmetric supercapacitors using holey graphene electrodes and redox electrolytes, *Carbon* 157 (2020) 298-307.
- [30] Y. Zhang, Q. Wan, N. Yang, Recent advances of porous graphene: synthesis, functionalization, and electrochemical applications, *Small* 15 (2019) 1903780.
- [31] J. Gao, S. He, A. Nag, Electrochemical detection of glucose molecules using laser-induced graphene sensors: a review, *Sensors* 21 (2021) 2818.
- [32] F. Cui, H. Sun, X. Yang, H. Zhou, Y. Wu, J. Li, H. Li, J. Liu, C. Zeng, B. Qu, J. Zhang, Q. Zhou, Laser-induced graphene (LIG)-based Au@CuO/V<sub>2</sub>CT<sub>x</sub> MXene non-enzymatic electrochemical sensors for the urine glucose test, *Chem. Eng. J.* 457 (2023) 141303.

- [33] B.E. Nugba, N.O. Mousa, A. Osman, A.A. El-Moneim, Non-enzymatic amperometric biosensor with anchored Ni nanoparticles for urinary glucose quantification, *Diam. Relat. Mater.* 137 (2023) 110171.
- [34] R. Cao, J. Zhang, D. Wang, F. Sun, N. Li, J. Li, Electrodeposition cobalt sulfide nanosheet on laser-induced graphene as capacitive deionization electrodes for uranium adsorption, *Chem. Eng. J.* 461 (2023) 142080.
- [35] G. Yuan, T. Wan, A. BaQais, Y. Mu, D. Cui, M.A. Amin, X. Li, B.B. Xu, X. Zhu, H. Algadi, H. Li, P. Wasnik, N. Lu, Z. Guo, H. Wei, B. Cheng, Boron and fluorine Co-doped laser-induced graphene towards high-performance micro-supercapacitors, *Carbon* 212 (2023) 118101.
- [36] G. Yang, J. Liu, M. Zhou, J. Bai, X. Bo, Fast and facile room-temperature synthesis of MOF-derived Co nanoparticle/nitrogen-doped porous graphene in air atmosphere for overall water splitting, *ACS Sustainable Chem. Eng.* 8 (2020) 11947–11955.
- [37] I. Khan, N. Baig, A. Bake, M. Haroon, M. Ashraf, A. Al-Saadi, M.N. Tahi, S. Wooh, Robust electrocatalysts decorated three-dimensional laser-induced graphene for selective alkaline OER and HER, *Carbon* 213 (2023) 118292.
- [38] Y. Wang, H. Guo, M. Yuan, J. Yu, Z. Wang, X. Chen, One-step laser synthesis platinum nanostructured 3D porous graphene: a flexible dual-functional electrochemical biosensor for glucose and pH detection in human perspiration, *Talanta* 257 (2023) 124362.
- [39] T.S. Gopal, J.T. James, B. Gunaseelan, K. Ramesh, V. Raghavan, C.J.A. Malathi, K. Amarnath, V.G. Kumar, S.J. Rajasekaran, S. Pandiaraj, M.R. Muthumareeswaran, S. Pitchaimuthu, C. Abeykoon, A.N. Alodhayb, A.N. Grace, MXene-embedded porous carbon-based Cu<sub>2</sub>O nanocomposites for non-enzymatic glucose sensors, *ACS Omega* 9 (2024) 8448-8456.
- [40] A.K. Thakur, P. Sengodu, A.H. Jadhav, M. Malmali, Manganese carbonate/laser-induced graphene composite for glucose sensing, *ACS Omega* 9 (2024) 7869-7880.
- [41] A.G. Mohammad, S. Abbas, G. Zeynab, M. Faranak, G. Ali, Non-enzymatic glucose electrochemical sensor based on nitrogen-doped graphene modified with polyaniline and Fe<sub>3</sub>O<sub>4</sub>@MIL-101-NH<sub>2</sub> nano framework, *Inorg. Chem Commun.* 159 (2024) 111812.
- [42] S. Zhang, W. Zhao, C. Liu, J. Zeng, Z. He, C. Wang, W. Yuan, Q. Wang, Flower-

- like CoO nanowire-decorated Ni foam: A non-invasive electrochemical biosensor for glucose detection in human saliva, *Appl. Mater. Today* 36 (2024) 102083.
- [43] W. Qin, L. He, Y. Zhang, B. Li, L. Han, Y. Xu, Synchronous wrapping and inward-etching strategy on constructing yolk-shell MIL-88A@NiFe-PB heterostructures for electrochemical non-enzymatic glucose detection, *Microchem. J.* 196 (2024) 109641.
- [44] Y.-T. Xue, Z. Chen, X. Chen, G.-C. Han, X.-Z. Feng, H.-B. Kraatz, Enzyme-free glucose sensor based on electrodeposition of multi-walled carbon nanotubes and Zn-based metal framework-modified gold electrode at low potential, *Electrochim. Acta.* 483 (2024) 144009.
- [45] M. Chang, L. Hao, X. Li, H. Wang, N. Fu, Y. Zhang, Boosting the performance of enzyme-free biosensing system with Ni-Co bimetallic nanorod anchored on macroporous carbon composites for glucose monitoring, *Mater. Res. Bull.* 169 (2024) 112541.
- [46] K.-A. Zeinab, N. Leila, S. Saeed, CuCoP@Cu(OH)<sub>2</sub> core-shell nanostructure as a robust electrochemical sensor for glucose detection in biological and beverage samples, *Microchem. J.* 200 (2024) 110369.
- [47] M.Y. Ali, H.B. Abdulrahman, W.-T. Ting, M.M.R. Howlader, Green synthesized gold nanoparticles and CuO-based nonenzymatic sensor for saliva glucose monitoring, *RSC. Adv.* 14 (2024) 577-588.
- [48] W. Pan, Z. Zheng, X. Wu, J. Gao, Y. Liu, Q. Yuan, W. Gan, Facile synthesis of 2D/3D hierarchical NiCu bimetallic MOF for non-enzymatic glucose sensor, *Microchem. J.* 170 (2021) 106652.
- [49] Z. Xu, Q. Wang, H. Zhangsun, S. Zhao, Y. Zhao, L. Wang, Carbon cloth-supported nanorod-like conductive Ni/Co bimetal MOF: A stable and high-performance enzyme-free electrochemical sensor for determination of glucose in serum and beverage, *Food. Chem.* 349 (2021) 129202.
- [50] Y. Tian, X. Liu, Y. Geng, J. Wang, M. Ma, In-situ synthesis of self-supporting conductive CuCo-based bimetal organic framework for sensitive nonenzymatic glucose sensing in serum and beverage, *Food Chem.* 437 (2024) 137875.
- [51] X. Chen, X.-Z. Feng, T. Zhan, Y.-T. Xue, H.-X. Li, G.-C. Han, Z. Chen, H.-B. Kraatz, Construction of a portable enzyme-free electrochemical glucose detection system based on the synergistic interaction of Cu-MOF and PtNPs, *Sensor. Actuat. B-Chem.* 395 (2023) 134498.

[52] F. Zhou, H. Zhao, K. Chen, S. Cao, Z. Shi, M. Lan, Flexible electrochemical sensor with Fe/Co bimetallic oxides for sensitive analysis of glucose in human tears, *Anal. Chim. Acta* 1243 (2023) 340781.